Dynamic Bipedal Locomotion over Stochastic Discrete Terrain

Quan Nguyen, Ayush Agrawal, William Martin, Hartmut Geyer, and Koushil Sreenath.

***Abstract*—Due to their morphology and mechanical design, bipedal robots have the ability to traverse over a wide range of terrain including those with discrete footholds like stepping stones. This paper addresses the challenge of planar dynamic robotic walking over stochastically generated stepping stones with significant variations in step length and step height, and where the robot has knowledge about the location of the next discrete foothold only one step ahead. Specifically, our approach utilizes a 2-step periodic gait optimization technique to build a library of gaits parametrized by their resulting step lengths and step heights, as well as the initial configuration of the robot. By doing so, we address the problems involved during step transition when switching between the different walking gaits. We then use gait interpolation in real-time to obtain the desired gait. The proposed method is successfully validated on ATRIAS, an underactuated, human-scale bipedal robot, to achieve precise footstep placement. With no change in step height, step lengths are varied in the range of [23:78] cm. When both step length and step height are changed, their variation are within [30:65] cm and [-22:22] cm respectively. The average walking speed of both these experiments is 0.6 m/s.**

(a) Stepping stones with step length variation.

(b) Cinder block terrain with step length variation.

(c) Stepping stones with step length and step height variation.

Fig. 1: ATRIAS walking over stepping stones. Experimental video: https://youtu.be/JKkPWHm6H7k https://youtu.be/jQeC1OOmOmk. Simulation video: https://youtu.be/Pxhb4_ojiC8.

I. Introduction

A primary advantage of legged robotic systems over their wheeled counterparts is their ability to navigate over rugged terrain such as over discrete footholds or "stepping stones". Unlike prior work that rely on simplistic robot models (such as pendulum models) and fully-actuated control schemes (e.g. ZMP) to achieve the desired foot placements, in this work, we propose a formal framework that achieves planar dynamic underactuated walking over a randomly varying discrete terrain with significant simultaneous changes in step length and step height at each step.

Early work on footstep control relied on fully actuated bipedal robots (Kajita, Kanehiro, Kaneko, Fujiwara, Harada, Yokoi and Hirukawa, 2003),(Kuffner, Nishiwaki, Kagami, Inaba and Inoue, 2001),(Chestnutt, Lau, Cheung, Kuffner, Hodgins and Kanade, 2005). In the context of footstep planning for bipedal robot navigation in cluttered environments, impressive results have been achieved in (Michel, Chestnutt, Kuffner and Kanade, 2005), (Chestnutt, Kuffner, Nishiwaki and Kagami, 2003), and (Nishiwaki, Chestnutt and Kagami, 2012) using vision and laser-range sensors. Several new methods for legged

The work by Q. Nguyen, A. Agrawal, and K. Sreenath is supported by NSF grant IIS-1526515 and departmental startup funds. The work by W. Martin and H. Geyer is supported by NSF grant CNS-1239143.

Q. Nguyen is with the Dept. of Mechanical Engineering, Carnegie Mellon University, Pittsburgh, PA 15213, email: quannguyen@cmu.edu.

A. Agrawal and K. Sreenath are with the Dept. of Mechanical Engineering, University of California, Berkeley, CA 94720, email: {ayush.agrawal,koushils}@berkeley.edu.

W. C. Martin and H. Geyer are with the Robotics Institute, Carnegie Mellon University, Pittsburgh, PA 15213, email: {wmartin,hgeyer}@cmu.edu.

This paper is an invited journal version of our prior work in (Nguyen, Agrawal, Da, Martin, Geyer, Grizzle and Sreenath, 2017).

robot control emerged from the DARPA Robotics Challenge in 2015, some based on mixed-integer quadratic programs (Deits and Tedrake, 2014). However, as mentioned in (Deits, 2014, Chap. 4), mixed-integer-based footstep planning does not guarantee dynamic feasibility even on simplified robot models. These methods are therefore not applicable for dynamic walking with faster walking gaits in high degree-of-freedom underactuated robots. The approach developed in (Yang, Westervelt, Serrani and Schmiedeler, 2009), on the other hand, allows for aperiodic gaits by switching between multiple dynamically-feasible gaits, designed on a complete dynamical model. Although such a method could potentially be used for walking with varying step lengths, this method, however, requires *a priori* design of controllers that realize precise transitions between each pair of elements of the gait library, resulting in exponential (factorial) growth in the number of pre-designed controllers. In this work, we use tools from trajectory optimization to build a library of periodic walking gaits. Specifically, we use the direct collocation method to compute optimal state-action trajectories. In the context of hybrid systems and bipedal robots, the direct collocation methods have been utilized in recent work (Hereid, Cousineau, Hubicki and Ames, 2016; Gurriet, Finet, Boeris, Hereid, Harib, Masselin, Grizzle and Ames, 2017). Moreover, optimization-based techniques have been widely used in bipedal robotic locomotion literature (Feng, Whitman, Xinjilefu and Atkeson, 2015; Kuindersma, Permenter and Tedrake, 2014; Dai, Valenzuela and Tedrake, 2014).

Instead of relying on simplified dynamical models, such as the linear inverted pendulum with massless legs (Desai and Geyer, 2012),(Rutschmann, Satzinger, Byl and Byl, 2012), this method utilizes a novel control strategy based on the full nonlinear hybrid dynamic model of the underactuated robot to achieve precise foot placement with single-step changes on step length and step height. We begin by pre-computing a library consisting of a small number of periodic gaits that are parametrized by initial and final values of their step lengths and step heights and have a periodic gait comprising of two walking steps (see Fig. 8). These gaits satisfy torque limits, constraints on ground reaction forces and other physical constraints. Instead of pre-computing transition controllers between the different gaits in the library, the gait library is linearly interpolated based on the desired footstep placement of the next stepping stone as well as on the robots current configuration, to compute a desired gait. This work builds off recent work on periodic walking gait libraries in (Da, Harib, Hartley, Griffin and Grizzle, 2016; Da, Hartley and Grizzle, 2017). In comparison to prior work, this paper makes the following additional contributions:

- We present 2-step periodic gait optimization and a gait-library-interpolation approach for achieving a continuum of desired step lengths and step heights.
- 2-step periodic gait optimization takes into account not only the footstep placement of the next step but also current configuration of the robot, allowing us to handle the step transition when switching between different walking gaits.

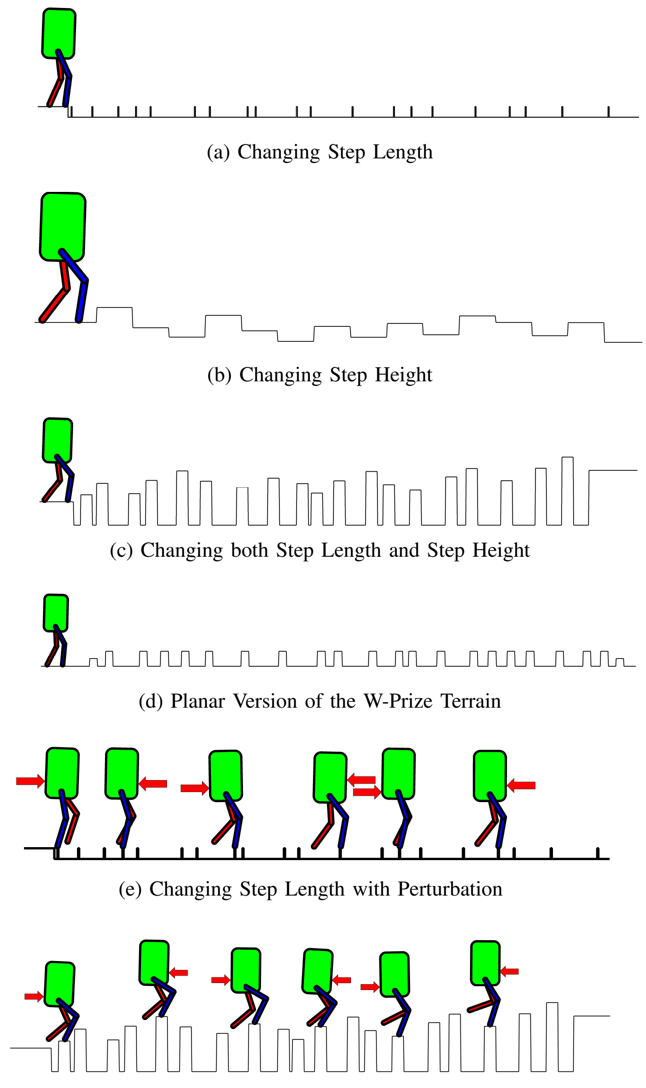

(a) Changing Step Length

(b) Changing Step Height

(c) Changing both Step Length and Step Height

(d) Planar Version of the W-Prize Terrain

(e) Changing Step Length with Perturbation

(f) Changing both Step Length an Step Height with Perturbation

Fig. 2: The problem of dynamically walking over a randomly generated set of discrete footholds. Simulation video: https://youtu.be/Pxhb4_ojiC8.

- Numerical validations on different terrains (see Fig. 2).
- Experimental validation on ATRIAS robot (see Fig. 1) for the problem of:
  - changing step length within the range of $[23:78]$ cm.
  - changing both step length and step height in the range of $[35:60]$ cm and $[-22:22]$ cm respectively.

A list of simulation and experiment videos is provided in Table. I.

With respect to our prior work in (Nguyen, Agrawal, Da, Martin, Geyer, Grizzle and Sreenath, 2017), this paper presents experiments on navigating over cinder block terrain with step length variation; stepping stone terrain with simultaneous variation in step length and step height; detailed information on the experimental setup, walking gait optimization and controller implementation; and preliminary results on using vision for determining step length.

We believe that this is the first work that successfully experimentally demonstrates the problem of *dynamic walking* on

TABLE I: List of simulation and experiment videos in the paper.

1.	Simulation video	https://youtu.be/Pxhb4_ojiC8.
2.	Experiment video of ATRIAS walking on rubber tiles	https://youtu.be/JKkPWHm6H7k
3.	Experiment of ATRIAS walking on cinder blocks with (a) variation of step length; (b) simultaneous variation of step length and step height; and (c) preliminary experiment of ATRIAS walking on stepping stones with an on-board camera.	https://youtu.be/jQeC1OOmOmk

stepping stones with simultaneous variation in step length and step height for a bipedal or humanoid robot. Our experiment handles simultaneous changes in step length and step height at an average walking speed of 0.6 m/s.

The remainder of the paper is organized as follows. Section II presents the hybrid dynamical model of 2D ATRIAS, an underactuated planar bipedal robot. Section III presents background on periodic gait optimization using Hybrid Zero Dynamics and input-ouput linearizing controller. Section IV presents our proposed approach on 2-step periodic gait optimization and a gait library interpolation strategy. Section V presents numerical validation of the controller on ATRIAS model. Section VI presents experimental validation of ATRIAS robot walking on stepping stones. Section VII introduces preliminary results towards future work on dynamic walking over stepping stones with an on-board camera. Finally, Section VIII provides concluding remarks.

II. Dynamical Model for Walking

Fig. 3 illustrates the 2D representation of ATRIAS. Its total mass is 63 kg, with approximately 50% of the mass in the hips and 40% in the torso, and with light legs formed by a four-bar linkage. The robot is approximately left-right symmetric.

Ignoring the compliance in the system, the configuration variables for the system can be defined as $q := (q_T, q_{1R}, q_{2R}, q_{1L}, q_{2L}) \in \mathbb{R}^5$. The variable q_T corresponds to the world frame pitch angle, while the variables $(q_{1R}, q_{2R}, q_{1L}, q_{2L})$ refer to the body coordinates for linkages. The subscripts L and R refers to left and right legs. Fig. 3 illustrates q_1, q_2 angles for one of the legs. Each of the four linkages are actuated by a DC motor behind a 50:1 gear ratio harmonic drive, with the robot having one degree of underactuation. The four-bar linkage mechanism comprising of the leg coordinates (q_1, q_2) map to the leg angle and knee angle (q_{LA}, q_{KA}), as $q_{LA} := \frac{1}{2}(q_1 + q_2)$ and $q_{KA} := q_2 - q_1$. A simple transformation then relates the leg coordinates to the leg and knee angles,

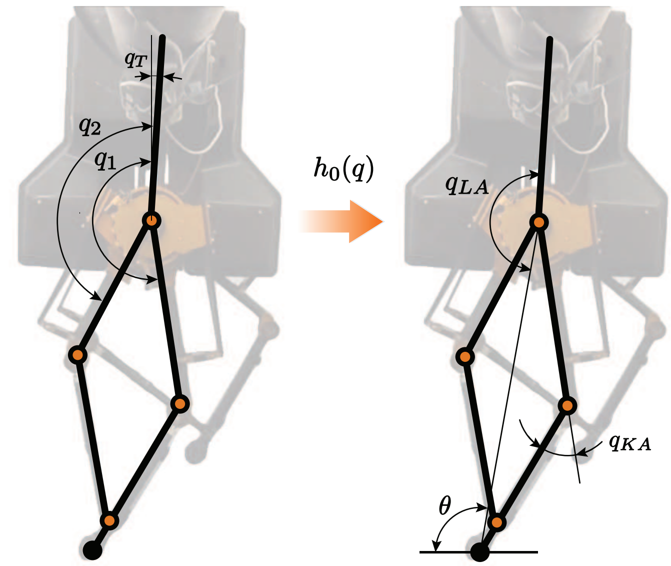

Fig. 3: Biped coordinates and outputs. The world frame pitch angle is denoted by q_T, while (q_1, q_2) are body coordinates. The outputs to be controlled are denoted by q_{LA} and q_{KA}. The model is assumed left-right symmetric.

$$h_0(q) = \begin{bmatrix} \frac{1}{2} & \frac{1}{2} & 0 & 0 \\ 0 & 0 & \frac{1}{2} & \frac{1}{2} \\ -1 & 1 & 0 & 0 \\ 0 & 0 & -1 & 1 \end{bmatrix} \begin{bmatrix} q_1^{st} \\ q_2^{st} \\ q_1^{sw} \\ q_2^{sw} \end{bmatrix} =: \begin{bmatrix} q_{LA}^{st} \\ q_{KA}^{st} \\ q_{LA}^{sw} \\ q_{KA}^{sw} \end{bmatrix}, \qquad (1)$$

where the indices st and sw are used to denote stance or swing legs respectively.

The state x denotes the generalized positions and velocities of the robot and u denotes the joint torques. A hybrid model of walking can be expressed as

$$\begin{cases} \dot{x} &= f(x) + g(x)u \quad x \notin \mathcal{S} \\ x^+ &= \Delta(x^-) \quad\quad\quad\; x \in \mathcal{S}, \end{cases} \qquad (2)$$

where $\mathcal{S}$ is the impact surface and Δ is the reset or impact map. A more complete description of the robot and a derivation of its model are given in (Ramezani, Hurst, Akbari Hamed and Grizzle, 2014).

III. Periodic Walking with Hybrid Zero Dynamics

Having described the dynamical model of ATRIAS, we now preset a brief overview of the Hybrid Zero Dynamics framework to design periodic gaits and feedback controllers to achieve stable, dynamic walking on ATRIAS. We begin by describing the periodic gait generation process, which can be posed as a nonlinear optimization program. We then present the input-output linearizing controller, that stabilizes the periodic walking gaits.

A. Periodic Gait Design Using Virtual Constraints

The nominal feedback controller is based on the Hybrid Zero Dynamics framework and virtual constraints presented in (Westervelt, Grizzle, Chevallereau, Choi and Morris, 2007).

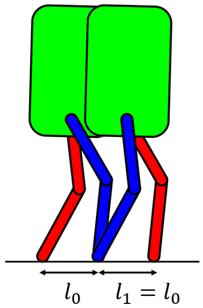

Fig. 4: Periodic walking gait has the resulting step length (l_1) similar to the initial step length (l_0), or in other words $l_1 = l_0$.

Virtual constraints are kinematic relations that synchronize the evolution of the robot's coordinates via continuous-time feedback control. One virtual constraint in the form of a parametrized spline can be imposed for each (independent) actuator. Parameter optimization is used to find the spline coefficients so as to create a periodic orbit satisfying a desired step length, while respecting physical constraints on torque, motor velocity, and friction cone. Since the gait is periodic, the initial step length and the resulting step length must be the same (see Fig. 4). The optimizer used here is based on the direct collocation framework from (Jones, 2014), although other optimization methods, such as (Hereid, Hubicki, Cousineau, Hurst and Ames, 2015) or `fmincon` can be used as well.

The virtual constraints are expressed as an output vector

$$y = h_0(q) - h_d(s(q), \alpha), \tag{3}$$

to be asymptotically zeroed by a feedback controller. Here, $h_0(q)$ specifies the quantities to be controlled and $h_d(s, \alpha)$ is a 4-vector of Beziér polynomials in the parameters α specifying the desired evolution of the $h_0(q)$, where s is a gait phasing variable defined as

$$s := \frac{\theta - \theta_{init}}{\theta_{final} - \theta_{init}}, \tag{4}$$

with $\theta = q_T + q_{LA}^{st}$ being the absolute stance leg angle. θ_{init} and θ_{final} are the initial and final values of the absolute leg angle at the start and end of a walking step and are obtained through the optimization problem described in this section.

The cost function and constraints for the optimization are formulated as in (Westervelt, Grizzle, Chevallereau, Choi and Morris, 2007) [Chap. 6.6.2], with the constraints given in Table II and the cost taken as the integral of squared torques over step length:

$$J = \int_0^T ||u(t)||_2^2 \; dt. \tag{5}$$

In addition to the above constraints, we also need to guarantee the periodicity of the gait through the *periodicty constraints*:

- The initial state at start of the first step is given by $x = x_0^+$ with corresponding (initial) step length of l_0.
- The state at end of the first step (before impact) is given by $x = x_1^-$ with corresponding (resulting) step length of l_1.

TABLE II: Optimization constraints

Motor Torque	$\lvert u \rvert \leq 7$ Nm
Impact Impulse	$F_e \leq 15$ Ns
Friction Cone	$\left\lvert \frac{F_{st}^h}{F_{st}^v} \right\rvert \leq 0.6$
Vertical Ground Reaction Force	$F_{st}^v \geq 200$ N
Mid-step Swing Foot Clearance	$h_f\rvert_{s=0.5} \geq 0.1$ m

- Impact constraints at the end of the step are enforced as $x_1^+ = \Delta(x_1^-)$.
- Periodic constraints are then enforced as $x_1^+ = x_0^+$, resulting in $l_1 = l_0$.

Here, the superscript '$-$' and '$+$' represent the state right before and right after the impact, and Δ is the reset or impact map from (2).

To generate the 2-step-periodic walking gaits using direct collocation with the specifications mentioned above, we begin by discretizing each walking phase in time by a specified number of nodes N,

$$0 = t_0 < t_1 < t_2 < \cdots < t_N = T, \tag{6}$$

where T represents the time to impact. In particular, we use $N = 20$. Direct collocation then converts the original trajectory optimization problem,

$$\begin{aligned} J = \min_{u(t)} \quad & \int_0^T ||u(t)||_2^2 \; dt \\ \text{st.} \quad & x(t) = \int_0^t f(x(t)) + g(x(t))u(t)dt \\ & 0 \geq c(x(t), u(t)), \quad 0 \leq t \leq T, \end{aligned} \tag{7}$$

into that of a nonlinear program. Here, $c(x(t), u(t))$ represent the physical constraints described in Table II as well as *periodicity constraints*. This is achieved by approximating the state and control input trajectories by polynomial splines. In particular, we use the Hermite-Simpson algorithm, which approximates the integral expressions in (7) by piecewise quadratic functions, leading to the following nonlinear program,

$$J = \min_{u_i} \sum_{i=1}^{N-1} \frac{\Delta t_i}{6} \left(\|u_{i-1}\|^2 + 4\|u_i\|^2 + \|u_{i+1}\|^2 \right) \tag{8}$$

$$\begin{aligned} s.t. \quad & c(x_i, u_i) \leq 0, \quad 0 \leq i \leq N, \\ & x_{i+1} - x_{i-1} - \frac{\Delta t_i}{6} (\dot{x}_{i-1} + 4\dot{x}_i + \dot{x}_{i+1}) = 0, \\ & x_i - \frac{1}{2}(x_{i+1} + x_{i-1}) - \frac{\Delta t_i}{8}(\dot{x}_{i-1} - \dot{x}_{i+1}) = 0, \end{aligned}$$

where for all $i \in \{1, 3, \cdots, N-1\}$, $\Delta t_i = t_{i+1} - t_{i-1}$ is the time interval, x_i and u_i are the state and input respectively at node i, $\dot{x}_i$ is the derivative of the state at node i satisfying the dynamics given by $\dot{x}_i = f(x_i) + g(x_i)u_i$. The optimal state and input trajectories are then obtained by cubic and quadratic polynomial spline interpolation respectively. The desired output parameters α, θ_{init} and θ_{final} can be extracted from the optimal state trajectories through a simple Bézier curve fit. The nonlinear program in (8) can be solved using numerical NLP solvers such as `fmincon` or IPOPT. We refer the reader to (Hereid, Cousineau, Hubicki and Ames, 2016) for more details on the specifics of the trajectory optimization scheme.

B. Input-output linearization

The optimization results in a desired walking gait encoded through $h_d(s(q), \alpha)$ in (3). The goal for our controller, therefore, is to drive $y(q) \to 0$. In our method, we use an input-output linearizing controller, a nonlinear feedback controller to enforce exponential stability of the system (Ames, Galloway, Sreenath and Grizzle, 2014). If $y(q)$ has vector relative degree 2, then the second derivative takes the form

$$\ddot{y} = L_f^2 y(q, \dot{q}) + L_g L_f y(q, \dot{q})\ u. \tag{9}$$

We can then apply the following pre-control law

$$u(q, \dot{q}) = u^*(q, \dot{q}) + (L_g L_f y(q, \dot{q}))^{-1}\ \mu, \tag{10}$$

where

$$u^*(q, \dot{q}) := -(L_g L_f y(q, \dot{q}))^{-1} L_f^2 y(q, \dot{q}), \tag{11}$$

and μ is a stabilizing control to be chosen. Defining transverse variables $\eta = [y,\ \dot{y}]^T$, and using the IO linearization controller above with the pre-control law (10), we have,

$$\ddot{y} = \mu. \tag{12}$$

The exponential convergence of the control output y then can be easily derived using PD controller:

$$\mu = -K_p y - K_d \dot{y}. \tag{13}$$

In the following section, we introduce our proposed approach using 2-step periodic gait optimization to handle stochastically-varying discrete terrain resulting in consecutive changes in step length and step height at each walking step.

IV. 2-Step Periodic Gait Design

The 2-step periodic gait approach comprises of a library of periodic gaits, where each gait consists of two walking steps that are potentially different in terms of step length or step height. Thus, one can choose a gait by not only taking into account the desired footstep location of the next step but also the current configuration of the robot. This approach of using a 2-step periodic gait has been primarily been inspired by the issues arising from step transitions when walking over varying stepping stones (Nguyen, Da, Grizzle and Sreenath, 2016) and when switching between walking gaits. The method combines virtual constraints, parameter optimization, and an interpolation strategy for creating a continuum of gaits from a finite library of gaits. The notion of a 2-step periodic gait means that the robot states are designed to converge back to the initial condition after 2 walking steps.

We will first start off with the problem of changing step length only or walking on flat ground with varied step length. We will then look at the problem of changing step height only and finally we will look at simultaneous changes in step length and step height.

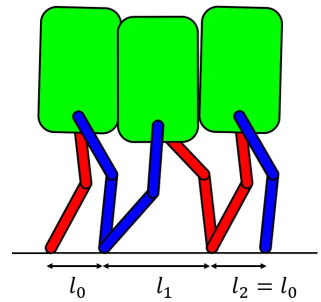

Fig. 5: 2-Step periodic walking with changing step lengths only. The walking gait is 2-step periodic therefore the step length of the second step and that of the initial condition are the same ($l_2 = l_0$).

1) Changing Only Step Lengths: In the nominal problem of periodic optimization presented in Section III-A, we need to optimize for only one walking step with the constraint on the resulting step length (l_1) to be equal to the initial step length (l_0) (see Fig. 4). For this problem, we use the same optimization framework discussed in III-A, but we will optimize for 2 walking steps while following additional constraints that allows us to have different step lengths for each of the steps in the 2-step periodic gait (see Fig. 5):

- The initial state at start of the first step is given by $x = x_0^+$with corresponding (initial) step length l_0.
- The state at the end of the first step (before impact) is $x = x_1^-$ with (resulting) step length l_1.
- Impact constraints at the end of the first step are enforced as $x_1^+ = \Delta(x_1^-)$.
- The initial state at start of the second step is given by $x = x_1^+$ with corresponding (initial) step length of l_1.
- The state at the end of the second step (before impact) is $x = x_2^-$ with (resulting) step length of l_2.
- Impact constraints at the end of the second step are enforced as $x_2^+ = \Delta(x_2^-)$.
- Periodic constraints are then enforced as $x_2^+ = x_0^+$, resulting in $l_2 = l_0$.

The optimization problem is then used to generate a gait library with different values of l_0 and l_1. In this work, we optimize four different gaits corresponding to:

$$\begin{cases} (l_0, l_1) = (0.3, 0.3) \text{ m} \\ (l_0, l_1) = (0.3, 0.7) \text{ m} \\ (l_0, l_1) = (0.7, 0.3) \text{ m} \\ (l_0, l_1) = (0.7, 0.7) \text{ m}. \end{cases} \tag{14}$$

This is similar to precomputing four gait primitives corresponding to walking with small steps ($(l_0, l_1) = (0.3, 0.3)$ m), switching from a small step to a large step ($(l_0, l_1) = (0.3, 0.7)$ m), switching from a large step to a small step ($(l_1, l_0) = (0.7, 0.3)$ m) and walking with large steps $(l_0, l_1) = (0.7, 0.7)$ m. Having a gait library with different gaits representing a few general motion primitives, we then do gait interpolation to get the desired walking gait with an arbitrary set of (l_0^d, l_1^d).

Let $\alpha(l_0^d, l_1^d)$ be the Beziér coefficients (defined in (3)) of the desired walking gait that has the initial step length

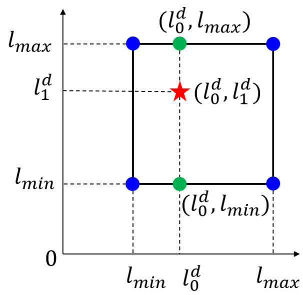

Fig. 6: Gait interpolation for the problem of changing step length only.

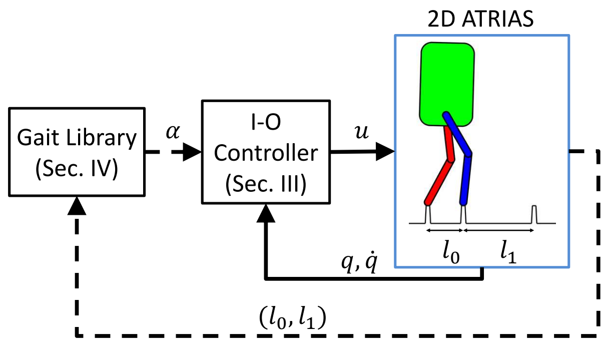

Fig. 7: Diagram of the controller structure for the problem of changing step length only, integrating the gait library and I-O linearization controller. Solid lines represent signals in continuous time; dashed lines represent signals in discrete time.

l_0^d and the resulting step length l_1^d. If $l_0^d \in [0.3 : 0.7]$ m and $l_1^d \in [0.3 : 0.7]$ m, we will compute $\alpha(l_0^d, l_1^d)$ using bilinear interpolation of the coefficients from the four nominal gait parameters precomputed using optimization. Therefore the new interpolated gait can be derived in real-time (within 1 ms in our experiment) right after the impact of each walking step. A detailed explanation for bilinear interpolation can be found in (Press, Teukolsky, Vetterling and Flannery, 1996), and summarized in Fig. 6. In this work, we use the MATLAB function `interp2` to implement the algorithm.

The gait library and bilinear interpolation are used to update the gait parameters α, θ_{init} and θ_{final} at the beginning of every walking step based on the desired footstep placement of the next step (l_1) and the step-length corresponding to the current configuration of the robot (l_0). They are then incorporated by the input-output linearizing controller 10 to control the robot to follow the updated walking gait. The closed-loop control diagram is shown in Fig. 7.

Remark 1: In our method, the desired trajectory $h^d(s, \alpha)$ in (3) represents a periodic gait of the robot and is a function of the gait phase variable s and the gait parameters described by the Bezier coefficient matrix α. For each gait, the gait phase variable is as defined in (4) and goes from 0 (at the beginning of the gait) to 1 (at the end of the gait). The Bezier polynomial with coefficients specified by α and evaluated at each point in the gait, $s \in [0, 1]$, provides the desired evolution of the actuated degrees-of-freedom. Thus, the interpolation between two gaits can be done by interpolating the two corresponding matrices of their gait parameters.

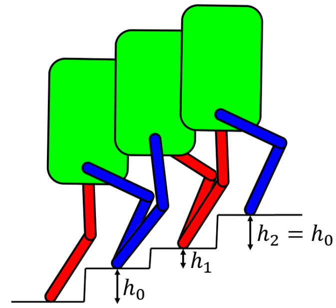

Fig. 8: 2-Step periodic walking with changing step heights only. The walking gait is 2-step periodic therefore the step height of the second step and that of the initial condition are the same ($h_2 = h_0$). Note that step heights h_0, h_1 can be positive (stepping up) or negative (stepping down). In this figure, we illustrate the case of both h_0 and h_1 being positive for convenience.

Remark 2: If l_0 or l_1 do not lie in the step length range of the designed gaits, then we can also use extrapolation to compute the gait parameters for the desired gait.

Remark 3: The proposed method has a resemblance to Model Predictive Control (MPC). While we use a 2-step periodic gait, we switch the gait at the end of each step, i.e., half-way into the 2-step periodic gait. For instance, with current step length being l_0, and subsequent step lengths being l_1, l_2, we use a gait with (l_0, l_1) and switch at the end of the first step to a gait (l_1, l_2) so that there is an overlap of one step between the gaits. The proposed method appears to easily address gait transitions that typically cause large violations in unilateral force constraints, friction constraints, and torque constraints. This is in contrast to the high rate of failure observed during gait transitions when using 1-step periodic gaits, see (Nguyen, Da, Grizzle and Sreenath, 2016, Table 2). While our method outperforms the 1-step gait library in (Nguyen, Da, Grizzle and Sreenath, 2016), it must be noted that we do not establish any formal guarantees for successful gait transitions.

Remark 4: Our prior work in (Nguyen, Da, Grizzle and Sreenath, 2016) used control barrier functions to handle gait transitions. In particular, as seen in (Nguyen, Da, Grizzle and Sreenath, 2016, Table 2), the addition of control barrier functions to a 1-step periodic gait library based method dramatically improves the success rate of walking over stochastic terrain. While this appears to work well, the feasibility of the quadratic program that enforces the control barrier constraint is not guaranteed. In this present work, as we will see, we achieve better results using the 2-step periodic gait library without using control barrier functions. We can easily add control barrier functions on top of the current method to further enforce and formally guarantee these safety-critical constraints. Since the underlying method achieves the foot placement without requiring the barriers, the barriers will remain inactive most of the time, leading to better feasibility of the quadratic program.

2) Changing Only Step Heights: For the problem of changing step heights only, the framework presented for changing

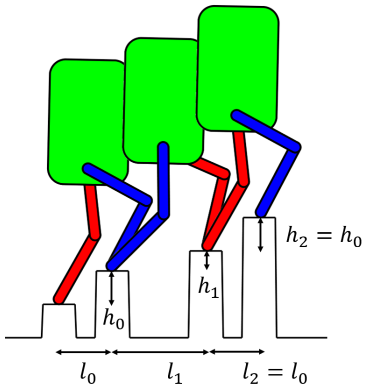

Fig. 9: 2-Step periodic walking with changing step lengths and step heights. The walking gait is 2-step periodic therefore the step length and step height of the second step and that of the initial condition are the same ($l_2 = l_0, h_2 = h_0$). Note that step heights h_0, h_1 can be positive (stepping up) or negative (stepping down). In this figure, we illustrate the case of both h_0 and h_1 being positive for convenience.

step length on flat ground in Section IV-1 can be applied where (h_0, h_1) plays the role of (l_0, l_1) (see Fig. 8). For this problem, we assume that stair tread length (horizontal distance from the edge of the stair to the stair riser) is constant. This translates to requiring the step length of our gait being constant. Subsequently, we generate four two-step periodic gaits with different step heights as done for the varying step length case in (14) and Fig. 6. Note that for optimizing gaits with step height variation, we will need to adjust the constraint on swing foot clearance stated in Table. (II), to avoid foot scuffing to the corners of the stair terrain (see Fig. 8).

3) Changing Both Step Lengths and Step Heights: We now can combine the methods presented in Section IV-1 and IV-2 to handle the problem of walking on stepping stones with varied step length and step height for every walking step (see Fig. 9). Since the gait parameters now depend on 4 variables l_0, h_0, l_1, h_1, the gait interpolation needs to be extended for 4 variables and the number of gaits increases to $2^4 = 16$ gaits.

Remark 5: Note that each of the nominal periodic walking gaits presented in Section III is locally exponentially stable (Westervelt, Grizzle, Chevallereau, Choi and Morris, 2007). The stability condition for switching policies between different locally exponentially stable periodic gaits can be found in (Motahar, Veer and Poulakakis, 2016), wherein it is assumed that one periodic gait switches into the domain of attraction of a subsequent periodic gait. With the 2-step periodic gaits, we can guarantee that when we switch to the next gait, the initial state of the robot is close to the periodic orbit of the next gait.

V. Numerical Validation

Having presented our approach of using a 2-step periodic gait library, we now demonstrate the effectiveness of the proposed method by conducting numerical simulations on the model of ATRIAS.

Using our method, we can control our robot to traverse over different type of terrains:

- Changing step length only within the range of [20:90] cm with the precision of only 2 cm (see Fig. 2a)
- Changing step height only within the range of [-30:30] cm where the step length is constant at 50 cm (see Fig. 2b)
- Changing step length and step height at the same time where the range of step length and step height are [30:80] cm and [-30:30] cm respectively (see Fig. 2c)
- Planar version of the W-Prize terrain (W-Prize, 2009) (see Fig. 2c)
- Changing step length with perturbation (see Fig. 2e), where the perturbation is generated by applying horizontal external force of ± 300 N on the robot torso with the duration of $0.2s$ in the middle of some steps.
- Changing step length and step height with perturbation (see Fig. 2f), with similar type of perturbation mentioned above but the magnitude of the external force is now 200 N.

In all simulations, we check constraints on footstep placement, friction constraints and input saturation stated in Table II. Note that friction constraints are checked for both impulse at impact and contact force during the continuous phase. Fig. 11 shows the satisfactions of those constraints in one example of ATRIAS walking on randomly generated discrete footholds shown in Fig. 2c, where step length and step height are varied in the range of [30:80] cm and [-30:30] cm respectively. In this simulation the absolute error between the desired step length and the real step length has the minimum of 0 m, the maximum of 0.0453 m and the mean of 0.0113 m.

With the problem of changing step length only, we also compare the performance of (a) our prior work on Control Barrier Functions and gait library presented in (Nguyen, Da, Grizzle and Sreenath, 2016) and (b) our proposed method of the 2-step periodic gait library. Both controllers are run on the same terrain illustrated in Fig. 2a. From Fig. 12, we can clearly see that our proposed method of 2-step periodic gait library (thick red line) has vertical ground reaction force (F^v_{st}) with smaller peak amplitudes, coefficient $k = |F^h_{st}/F^v_{st}|$ that remains further inside the friction cone, and control inputs with smaller norm. Note that although these two controllers are applied on the same terrain, the walking step times are different because the gait libraries and the low-level controllers are different.

In Fig. 10, we demonstrate the robot walking over multiple terrains including:

(1) Worst case of walking up and down with large step length,
(2) Worst case of walking up and down with small step length,
(3) 20 steps walking over randomly generated terrain with stone size of 25 cm,
(4) 20 steps walking over randomly generated terrain with stone size of 5 cm.

Note that we use the same controller with the same gait library for all these different terrains, thereby establishing that our single controller can handle different types of variation in the terrain, including step length, step height, as well as stone size.

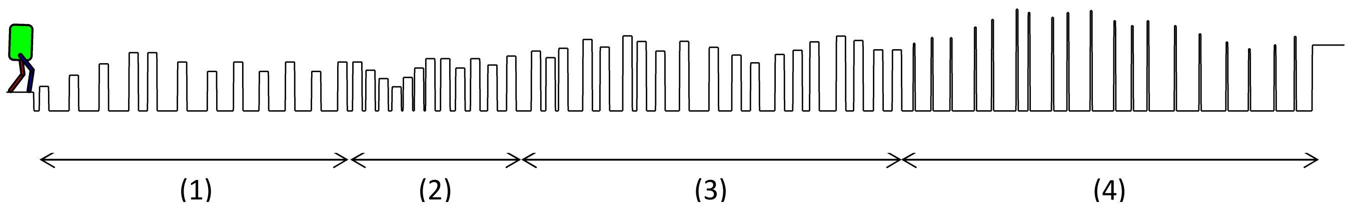

Fig. 10: ATRIAS walking on different terrains. (1) worst case of walking up and down with large step length. (2) worst case of walking up and down with small step length. (3) 20 walking steps over randomly generated terrain with stone size of 25 cm. (4) 20 walking steps over randomly generated terrain with stone size of 5 cm. Simulation video: https://youtu.be/Pxhb4_ojiC8.

In particular, with Terrain 4, the random terrain with stone size of 5 cm, we show the accuracy of the precise footstep placements. With Terrain 3, the random terrain with stone size of 25 cm, we show that the robot has a good swing foot clearance to avoid the corners of the larger stepping stones.

Here, we also sucessfully applied our proposed control method for the planar version of the W-Prize terrain listed in (W-Prize, 2009), which is made from placing cinder blocks with distances varied in $[35 : 98]$ cm. There are also stepping-up and stepping-down stones at the start and the end of the terrain (see Fig. 2d). Note that, in the simulation, all the physical constraints are checked except the constraint of avoiding the cinder blocks from tipping over. This additional challenge of the blocks tipping over is not addressed in this paper but it is an interesting problem to consider in future work.

In order to validate the robustness of the method, we generate perturbations in simulation by applying an external horizontal force, of magnitude ± 300 N and duration 0.2 s, to the robot's torso during walking over stepping stones (see Fig. 2e, 2f). From the simulations, we observe that our proposed method is robust to these perturbations. We believe the robustness arises since our method is based on virtual constraints and HZD, wherein feedback control is used to track desired trajectories that are functions of the gait phase variable instead of time (see Section III-A). The perturbation causes the rate of change of the gait phase variable to either increase or slow down, which causes a corresponding change in the desired trajectories. Thus, the final footstep location, which occurs when the swing foot has impact with the ground and the resulting gait phase variable reaches the final value ($s = 1$), is the same as the nominal one except for minor differences due to tracking errors. It must be noted that large perturbation forces in the backward direction could cause the phase variable to decrease and the robot to fall backwards, while large perturbation forces in the forward direction could result in violation of ground contact constraints.

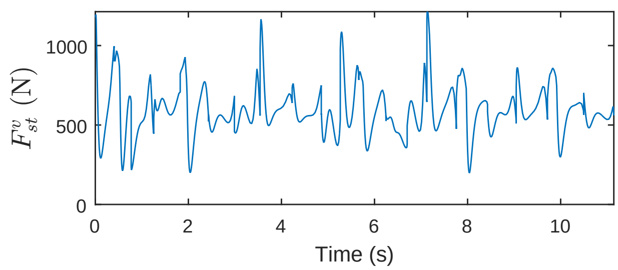

(a) Ground Reaction Force

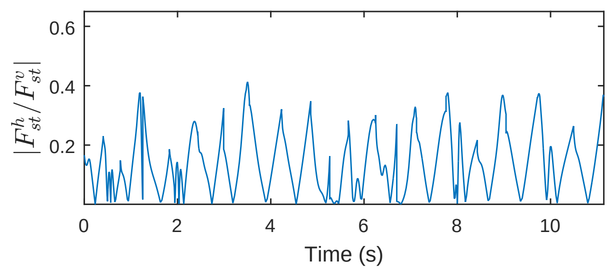

(b) Friction Cone

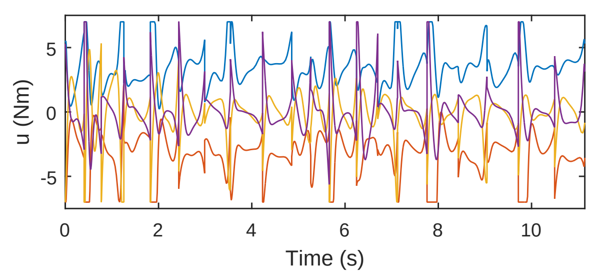

(c) Control Inputs

Fig. 11: Simulation of ATRIAS walking on randomly generated stepping stones with step length and step height changing in the range of [30:80] cm and [-30:30] cm respectively. The terrain is illustrated in Fig. 2c. The following constraints are enforced: (a) Ground reaction force: $F^v_{st} \geq 150$ N; (b) Friction cone: $|F^h_{st}/F^v_{st}| \leq 0.6$; and (c) Control motor inputs saturated at 7 Nm ($|u| \leq 7$). Note that there is a 50:1 gear ratio from the motors to the links.

VI. Experimental Validation

Having validated the controller in simulation, we now show the implementation of the proposed method on the robot hardware. We begin with a brief description of the robot hardware, followed by some implementation details. We then present the results for the following experiments:

- Changing step length within the range of $[23 : 78]$ cm.

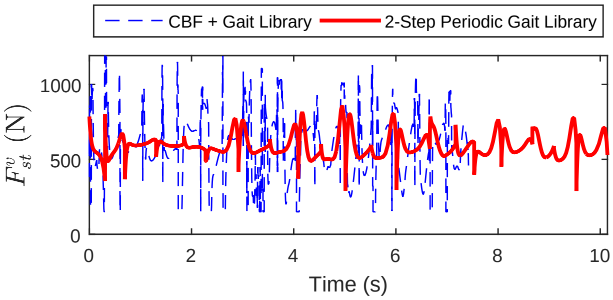

(a) Ground Reaction Force

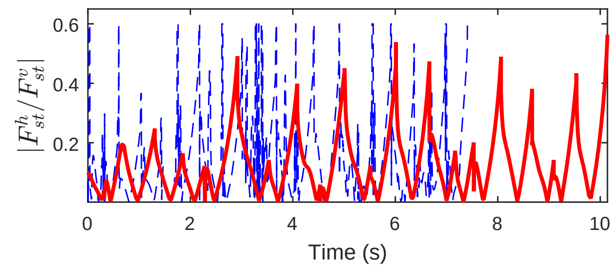

(b) Friction Cone

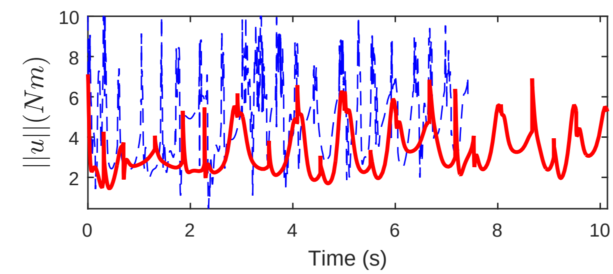

(c) Norm of Control Inputs

Fig. 12: We compare the "CBF + Gait Library" controller (dashed blue line) from (Nguyen, Da, Grizzle and Sreenath, 2016) with the proposed "2-Step Periodic Gait Library" controller (thick red line). As is seen, the proposed controller has better ground reaction force with smaller peak amplitudes, lower friction requirements, as well as smaller control inputs. The comparison is made by simulating both controllers for the same terrain illustrated in Fig. 2a.

- Changing both step length and step height in the range of $[35 : 60]$ cm and $[-22 : 22]$ cm respectively.

Remark 6: To build the required terrain in experiments, we stack a number of cinder blocks to change the terrain height. In doing so, an additional complexity arises in that these cinder blocks can topple over.

A. *Hardware Description*

ATRIAS is a 3D capable bipedal robot, equipped with three actuators on each leg – two motors ("leg motors") controlling the motion in the sagittal plane (q_1 and q_2 in Fig. 3) and one motor ("hip motor") controlling the lateral angle in the frontal plane (see Fig. 3). Therefore, to restrict the motion in the saggital plane, ATRIAS is attached to a boom (see Fig. 1b). The two leg motors in the saggital plane, connected to the front and rear thigh links through a 50:1 harmonic drive transmission and fiberglass plate springs, can be controlled to cause an effective change in leg length and/or leg angle. Further, in addition to the encoders mounted on the motor, ATRIAS is equipped with high-resolution (32-bit) absolute encoders for measuring joint angles and spring deflections. Position and orientation in the world frame are estimated using a high-precision inertial measurement unit (IMU). Table III lists the various quantities measured. Additionally, we define the body coordinates as $q_b := [q_1^{st}, q_2^{st}, q_1^{sw}, q_2^{sw}]^T$ and $\bar{q}_b := [\bar{q}_1^{st}, \bar{q}_2^{st}, \bar{q}_1^{sw}, \bar{q}_2^{sw}]^T$ corresponding to joint angles on the motor side and leg side respectively. See (Hubicki, Grimes, Jones, Renjewski, Spröwitz, Abate and Hurst, 2016) for further details on the ATRIAS bipedal robot platform.

TABLE III: Various measured quantities. The index $i \in \{st, sw\}$ represents stance/swing leg respectively.

Measured Quantity	Symbol	Sensor
Joint angles on motor side (i.e. at the output of the gears)	q_1^i, q_2^i	32-bit absolute optical encoders
Joint angles on leg side (i.e. at the output of the leaf-springs)	$\bar{q}_1^i$, $\bar{q}_2^i$	32-bit absolute optical encoders
Lateral joint angles (hip abduction)	q_3^i	13-bit absolute magnetic encoder
Torso Pitch	q_T	IMU
Robot Yaw	q_{yaw}^{robot}	IMU

B. *HZD Implementation*

The Hybrid Zero Dynamics framework is an elegant and powerful means to design gaits and develop model-based feedback controllers for underactuated dynamic bipedal locomotion. However, implementing the controller developed in Section III-B involves overcoming certain challenges.

In this section, we discuss some of the implementation details of the HZD controller on the ATRIAS robot. In particular, the 2D robot model is only used to generate a library of 2-step-periodic gaits (Section III). The outputs are then regulated using a PD controller. Fig. 13 shows an overview of the implemented controller on ATRIAS.

a) Phase Variable Computation: The phase variable s is computed using the joint angles measured at the output of the springs (i.e. on the leg side as opposed to the joint angles measured on the motor side). This is, in fact, the true phase variable with respect to the robot's base frame attached to the stance foot. Secondly, using joint measurements from the leg side leads to a "less noisy" phase variable. This is due to the fact that, during swing phase, the stance foot is assumed to be pinned to the ground (Westervelt, Grizzle, Chevallereau, Choi and Morris, 2007), i.e. stance foot is attached to the ground through an ideal revolute joint. This causes the motor side to oscillate (due to the compliant elements) with respect to the leg side and the robot's stance foot. Thus, using the joint angles from the motor side to compute the phase variable causes it to be oscillatory, which leads to oscillations in the desired outputs. This could in turn de-stabilize the system. To remove further noise from the signal, the computed phase variable is passed through a low-pass filter.

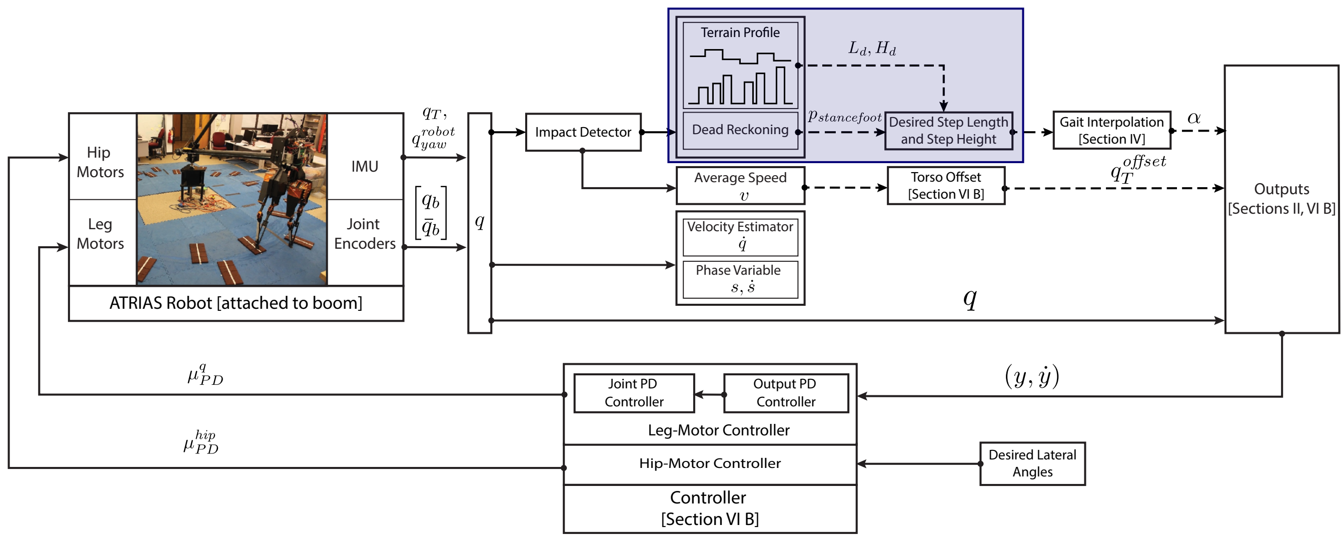

Fig. 13: Control Diagram of the implemented controller in experiment. Dashed lines denote discrete-time signals sampled at the beginning of every walking step. Continuous lines denote signals sampled at 1 kHz. The shaded blue block illustrates the computation of the desired step length and step height. In particular, we compute the desired step length and height based on the next step location obtained from the terrain profile and the current stance foot position, obtained from the robot yaw and forward kinematics (15). This entire block can essentially be replaced by a visual sensor.

b) Joint Velocity Computation: Joint velocities are obtained by first computing the finite difference of the motor encoder readings and then passed through a low-pass filter to remove high-frequency noise.

c) Dead Reckoning using IMU: The position of the robot in the world frame is estimated from a high-precision IMU mounted on the robot's torso. This information is then utilized to correct the relative distance between the robot's current stance foot and the next stepping stone (which is the desired step length input to the controller). In particular, we obtain an estimate of the robot's yaw with respect to an inertial frame. The robot's yaw, multiplied by the boom length, gives us an estimate of the robot's position,

$$p_{stancefoot} = q_{yaw}^{robot} \times l_{boom} + d_{hip\rightarrow stancefoot}, \qquad (15)$$

where q_{yaw}^{robot} is the yaw angle of the robot measured from the IMU signal, $l_{boom} = 2$ m is the boom length and $d_{hip\rightarrow stancefoot}$ is the distance from the hip to stance foot is computed based on the joint encoders. Note that we do not make use of any external sensors (such as a boom encoder or optical motion capture). The location of the stepping stones are precomputed and stored before the start of the experiment. However, only the distance between the current stepping stone and the next is provided to the controller one-step in advance. This distance is found based on where the robot is in the world (computed through IMU dead-reckoning) and corrected based on where the stance foot is on the current stone (computed through joint encoders).

d) Impact Detection: ATRIAS is not equipped with any force sensors or contact switches at the foot. To detect swing foot impacts on the ground, we use the leg axial force estimated by the spring compression (obtained by computing the difference in the encoder readings from the motor and leg sides). In particular, an impact is detected if the axial force as well as the phase variable s defined in (4) cross certain thresholds. Specifically, the we use a threshold value of 300 N for the axial force and 0.6 for the phase variable (see Fig. 14).

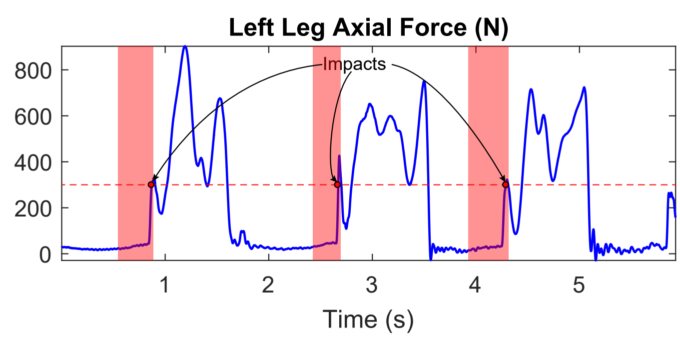

Fig. 14: Axial Forces on the Left Leg for six walking steps. Shaded red regions denote the periods when the phase variable is greater than the threshold value of 0.6. Dotted red line denotes the threshold value of the axial force at 300 N. An impact is detected when both, the axial force as well as the phase variable, cross their respective thresholds.

e) Control of Hip Motors: For simplicity, the desired lateral angles are kept constant, and enforced through a high gain position-derivative controller,

$$\mu_{PD}^{hip} = -K_p^{hip}\,(q_3 - q_{3,d}) - K_d^{hip}\,(\dot{q}_3 - \dot{q}_{3,d}), \qquad (16)$$

where $K_p^{hip},\ K_d^{hip} > 0$.

f) Walking Speed Regulation: We regulate the torso angle to maintain a desired average walking velocity – leaning the torso forward at the start of the swing phase causes the robot to accelerate and leaning the torso backwards causes it to decelerate. Torso angle regulation is achieved by changing the desired leg angles $h_d(s, \alpha)$ in (3) appropriately. In particular, at the start of swing phase, a desired torso offset is computed as,

$$q_T^{offset} = -K_p^T (v - v_d), \tag{17}$$

where v is the average forward velocity of the robot (estimated from the IMU) at the start of the swing phase, v_d is the desired average walking speed and $K_p^T > 0$. In our experiment, $v_d = 0.5\ m/s$ and $K_p^T = 0.1\ rad.s/m$. These values are tuned during the experiment of nominal periodic walking on flat ground and then used for other experiments. The offset computed above is bounded to prevent excessive torso oscillations.

The outputs y are then redefined as,

$$y = h_0(q) - h_d(s, \alpha) - q_T^{offset} \begin{bmatrix} 1 \\ 1 \\ 0 \\ 0 \end{bmatrix}. \tag{18}$$

g) Control of Leg Motors: A PD controller is utilized to regulate the outputs in (18). While the phase variable is computed using the joint angles on the leg side, the outputs y are computed using the joint angles on the motor side. The leg-motor torques are then computed using this output,

$$\mu_{PD}^y = -K_p y - K_d \dot{y} \tag{19}$$

This is done so that the leg motors do not work against the springs. The output PD controller in (19) is then mapped to the leg-joint torques using the transformation,

$$\mu_{PD}^q = h_0^{-1} (\mu_{PD}^y), \tag{20}$$

where h_0 is defined in (1).

C. Stepping Stone Experiment with Changing Step Length

In this Section, we will present experimental results on ATRIAS walking over stepping stones (see Fig.1). The circle is covered by 24 stepping stones with the following distances or desired step lengths of the robot:

$$\begin{aligned} L_d = [&56, 31, 64, 78, 33, 75, 30, 40, 72, 67, 35, 23, \\ &33, 52, 76, 50, 42, 78, 37, 31, 51, 76, 74, 69] \text{ cm}. \end{aligned} \tag{21}$$

The above step lengths were obtained randomly using the `rand` function in MATLAB. The controller is allowed knowledge of this information only for one step ahead.

Fig. 15 shows the experiment data including step length (the horizontal distance between swing and stance foot), the step length error (the error between the stance foot position and the center of the stone), the average speed of walking for each step and the joint torques of the right and left leg respectively. The step length errors have a mean of absolute of 3 cm and

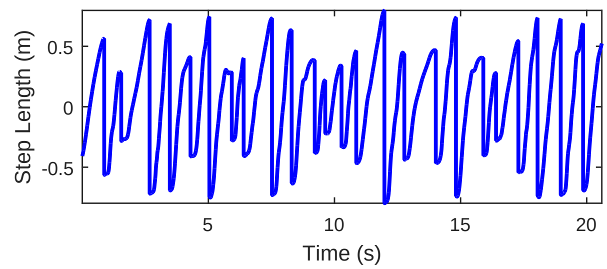

(a) Step Length

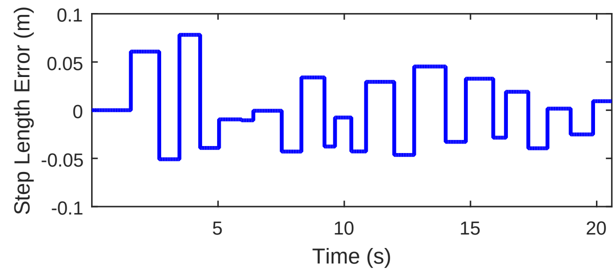

(b) Distance of the Foot from the Center of the Stone

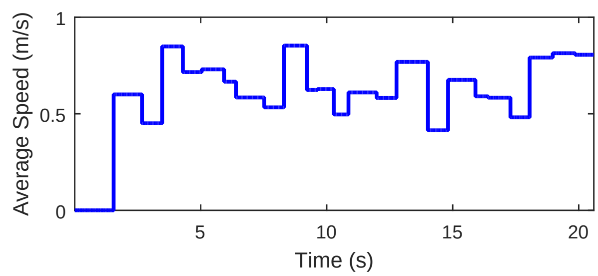

(c) Average Speed of each Walking Step

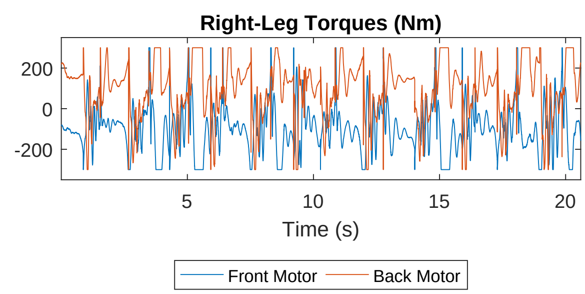

(d) Right-Leg Joint Torques

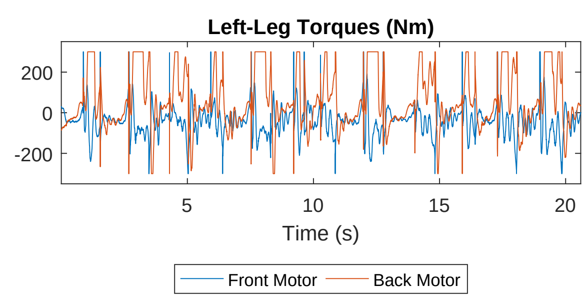

(e) Left-Leg Joint Torques

Fig. 15: Results from experiment of ATRIAS walking over stepping stones with changing step length (Fig. 1a). We present here the step length, step length error, average step speed, and joint torques. A video of the experiment can be found here: https://youtu.be/JKkPWHm6H7k.

absolute max of 7.8 cm and thus are always within the stone size of $[-10 : 10]$ cm. The experiment was conducted with input saturation of 5 Nm on the motor torques. This experiment thus validated the effectiveness of our proposed method for the problem of dynamic walking on stepping stones with a wide range of step length (within [23:78] cm) and at an average walking speed of 0.6 m/s over 24 steps taken by ATRIAS.

To better illustrate the problem, we also have the robot walking on cinder blocks (see Fig. 1b), where the height of the platform is 12 cm. Note that for this experiment, since the cinder blocks are not attached to the ground, we need to guarantee very accurate footstep placement and good friction constraint to ensure that the cinder blocks do not topple.

D. Stepping Stone Experiment with Changing Step Length and Step Height

For this experiment, the terrain was generated by placing 12 stepping stones (see Fig. 16) with different distances and heights. The following distances between these stones specify the desired step lengths:

$$L_d = [40, 35, 40, 60, 35, 60, 45, 35, 60, 35, 40, 50] \text{ cm}. \quad (22)$$

The heights of these stones from the ground are:

$$[12, 16, 38, 16, 32, 22, 12, 22, 32, 22, 16, 0] \text{ cm}, \quad (23)$$

that specifies the following step height changes between consecutive stepping stones:

$$H_d = [12, 4, 22, -22, 16, -10, -10, 10, -10, -6, -4, -12] \text{ cm}. \quad (24)$$

Similar to the previous problem of changing step length, we also report here in Fig. 17 the experiment data including step length (the horizontal distance between swing and stance foot), the step length error (the error between the stance foot position and the center of the stone), the average speed of walking for each step and the joint torques of the right and left leg respectively. The step length errors are just within $[-5 : 5]$ cm, therefore always staying inside stepping stones with the size of $[-10 : 10]$ cm. For this experiment, the change in step height is between -22 cm and $+22$ cm and the maximum height of the terrain to the ground is up to 38 cm. The average walking speed of the experiment is 0.6 m/s.

For the problem of changing both step length and step height in simulation, the initial and resulting step height in the gait library are selected from $\{-20, 20\}\, cm$ to represent stepping down and up, resulting in 16 $(= 2^2 \times 2^2)$ gaits for the gait library. Though this seems to work well in simulation, the knee angle of the stance leg tends to be large in all steps, leading to bad impacts that result in poor tracking in the subsequent step. In order to overcome this disadvantage, for the experiment, the zero step height is added to the set resulting in $\{-20, 0, 20\}\, cm$. This updated step height set represents a step down, flat ground, and step up respectively. Therefore, we need 36 $(= 2^2 \times 3^2)$ gaits in the gait library for the experiment of stepping stones with variation on both step length and height.

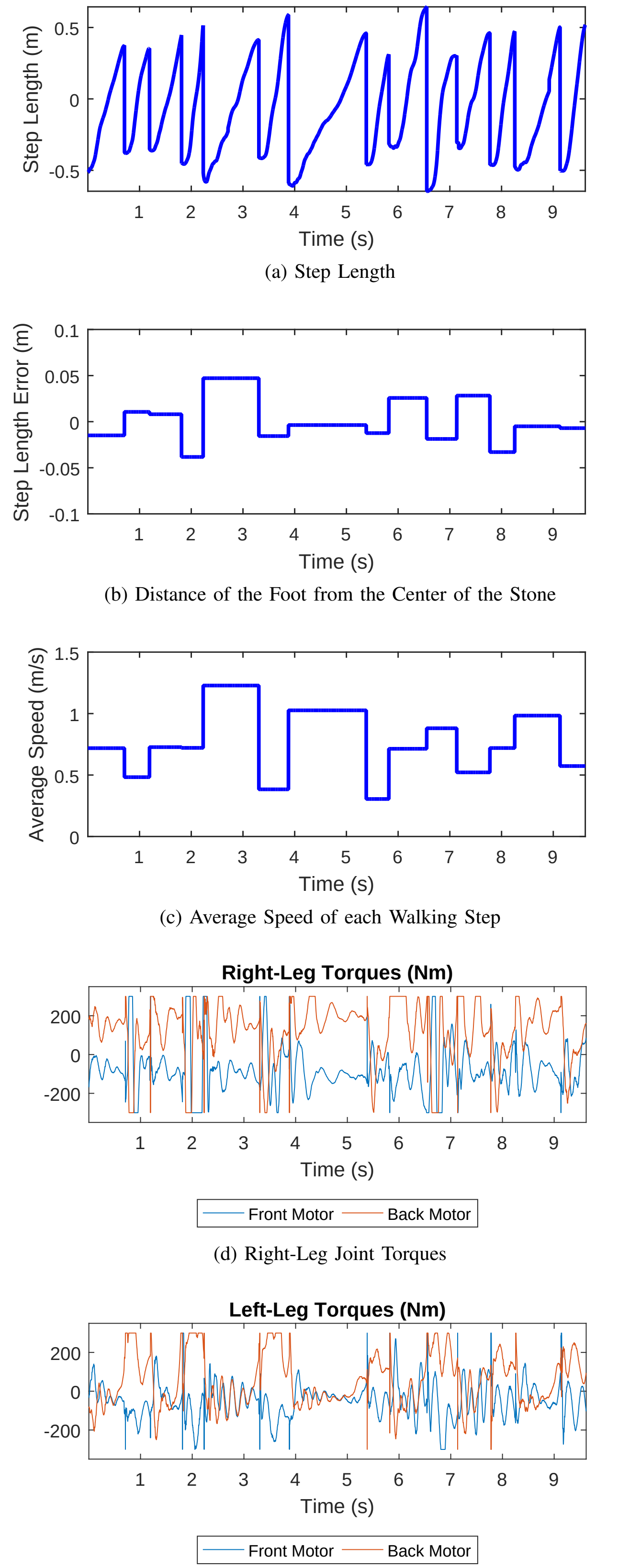

(a) Step Length

(b) Distance of the Foot from the Center of the Stone

(c) Average Speed of each Walking Step

(d) Right-Leg Joint Torques

(e) Left-Leg Joint Torques

Fig. 17: Results from experiment of ATRIAS walking over stepping stones with simultaneous changes in step length and step height (Fig. 1c). We present here the step length, step length error, average step speed, and joint torques. Experimental video: https://youtu.be/jQeC1OOmOmk.

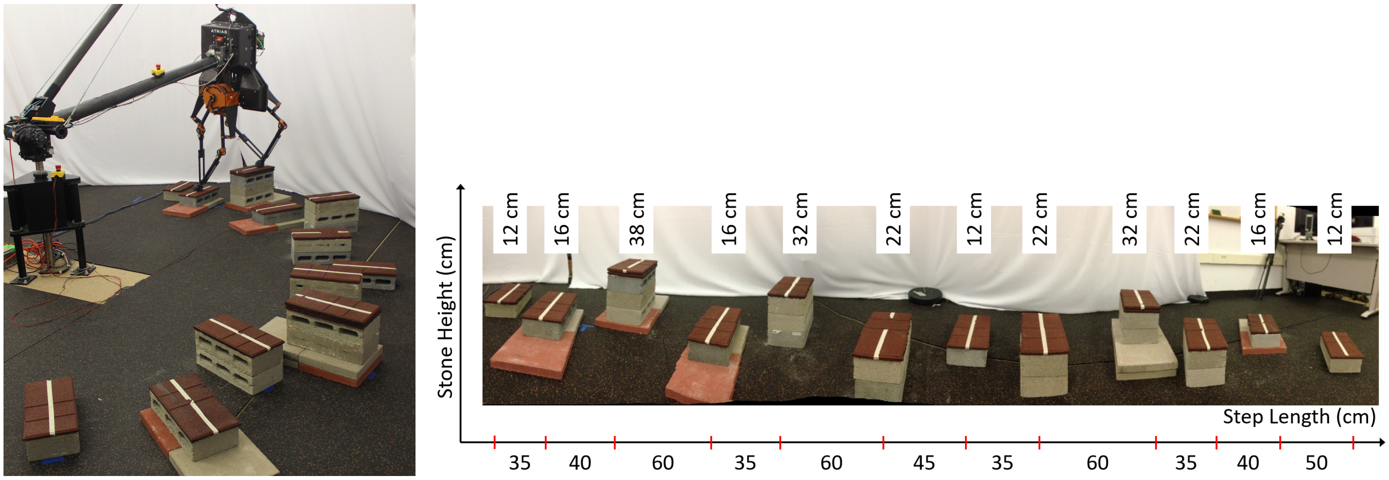

(a)

(b) a panorama of the terrain

Fig. 16: (a) ATRIAS stepping stone experiment with changing step length and step height. (b) Panorama of the terrain. Also shown are the step lengths between consecutive stones and the heights to the ground of each stone in the illustrated terrain. A video of the experiment can be found here: https://youtu.be/jQeC1OOmOmk

Note that cinder blocks used to create the terrain in Fig. 16 are not affixed to each other. Therefore, the accuracy of the footstep placement and good friction constraints are very critical to avoid both sliding and toppling issues in this experiment.

In the experiment shown in Fig.16, we tried to place the stepping stones so that we can test as much as possible different type of changes in the terrain. In addition to that, we also demonstrated our method on randomly generated terrains (see Fig. 18). For each test, the terrain is created by randomly placing 5 stepping stones, which corresponds to 6 walking steps with variation in both step length and step height. While the desired step lengths are randomly selected in increments of 1 cm, the stone heights are randomly selected from a limited discrete set due to the limitation of stone types used in the experiment. Furthermore, for the random height selection, we enforce the constraint that the starting and ending steps are at zero height so as to start and end the experiment on the ground level. The proposed method was successful on all eight random terrains that were attempted. Six of these are shown in the video and in Fig. 18.

Remark 7: In order to highlight the efficacy of the proposed method, we will discuss the footstep location range where the method was observed to work in simulations and in experiments. For the problem of changing step length only, with a gait library that is constructed for step lengths in the range [30:70] cm, the simulation works for step lengths in the range [20:90] cm – requiring both interpolation and extrapolation of the gait library. In experiment, due to model mismatch as well as the complexity of the real hardware, the step length range that the method can achieve is reduced to [23:78] cm. Similarly, for the problem of changing both step length and step height, while in simulation the robot can overcome the terrain with the step length and step height changing in the range of [30:80] cm and [-30:30] cm respectively, those ranges

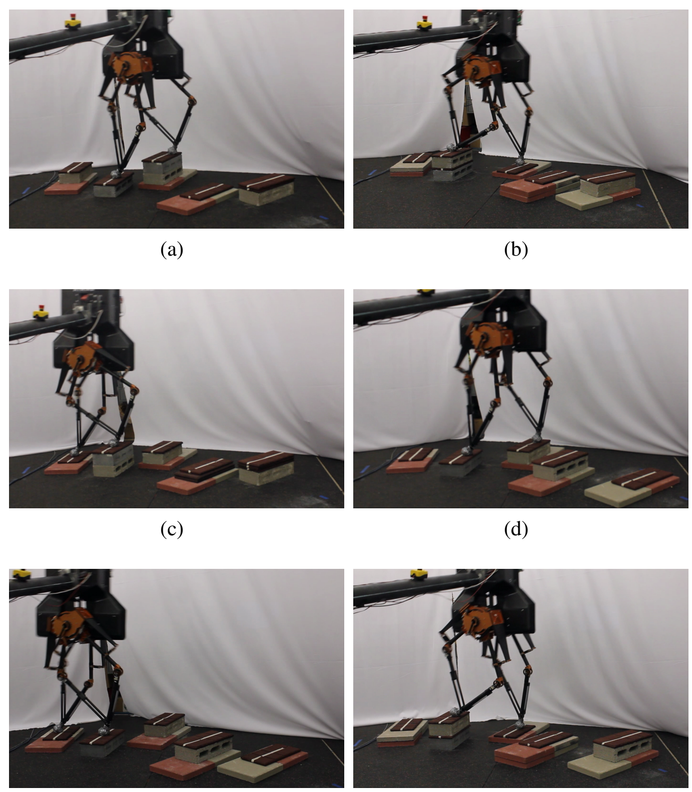

(a) (b) (c) (d) (e) (f)

Fig. 18: ATRIAS walking over different realizations of the stochastic terrain with simultaneous random variation in step length and step height.

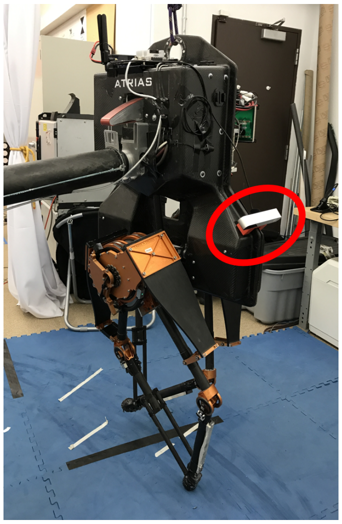

Fig. 19: On-board camera attachment on the ATRIAS robot.

(a) (b)

Fig. 20: Comparison of (a) real camera view and (b) camera scene after filtering.

are reduced to [35:60] cm and [-22:22] cm respectively in experiment. Note that, in order to construct the terrain for the experiment, we stack multiple cinder blocks together to change the terrain height (see Fig. 16), which can slide and topple over. This terrain setup requires the method to not only achieve an accurate footstep placement but also a conservative friction constraint. As a consequence, it further limits the performance of the method in experiments.

VII. Future Work

Having presented experiments validating the effectiveness of our proposed methodology, we now briefly discuss a few future research thrusts.

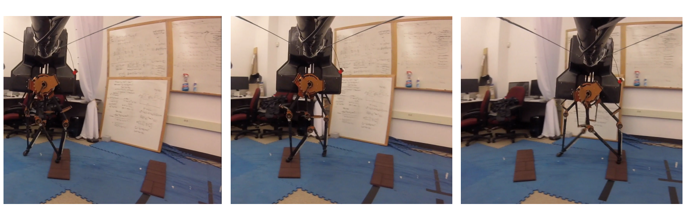

(a) (b) (c)

Fig. 21: Preliminary experiment on stepping stones using on-board camera. These are the snapshots of three consecutive walking steps.

We firstly present our preliminary experiment result toward future work on vision-based walking on stepping stones. Currently, in the experiments presented in the previous sections, we predefined the stone locations by measuring them at the start of the experiment and presenting this information to the controller one step ahead. For every walking step, the next stone location was then inputted to the controller right after an impact. As part of future work, we plan to use an on-board camera to determine the stone location rather than measuring them. It will help to show more clearly that our controller requires only one step ahead preview and can adapt to the change of stone location in real-time. This is also a step toward bringing the robot outdoor in the future.

For this work, we attempted to conduct some preliminary experiments using an on-board camera. Fig. 19 shows the camera attachment on the robot. The comparison of real camera view and camera scene after filtering is shown in Fig. 20. We successfully demonstrated a short experiment with three walking steps. Fig. 21 illustrates three snapshots of this experiment, where the desired step length is accurately determined using an on-board stereo camera. Due to delay in camera processing, there are still lots of cases when the camera processing give a wrong estimation of the distance between the camera to the stepping stones. A better synchronization solution between the robot and the camera could potentially compensate for the delay. Further results with a systematic development of the stereo algorithm will be tested and presented as part of future work. In an attempt to bring better perception for walking robots, we presented related result on synthetic vision for deep visual perception for dynamic walking on stepping stones in (Siravuru, Wang, Nguyen and Sreenath, 2017).

Additional future directions are also possible. We can formally analyze the stability for aperiodic walking obtained by switching among the gait library. We can study the conditions under which constraints that are satisfied by two individual gaits are still satisfied for the gait obtained through interpolation of the individual gaits. We can also extend the method to 3D walking, where the dimension of the problem will increase due to the requirement of changing step width as well.

VIII. Conclusion

We have presented a novel approach based on 2-step periodic gait optimization that allows us to handle a wide range of step lengths and heights with precise footstep placement. Since our walking gait optimization takes into account not only the upcoming terrain but also the current configuration of the robot, the method can effectively address the transition when the controller switches between different gaits. The gait library is pre-computed with a small number of gaits (4 gaits for the problem of changing step length or step height only and 16 gaits for the problem of changing both), then gait interpolation is implemented in real-time to adapt with random changes in the terrain as well as the initial condition of the robot. We successfully validated the proposed approach on ATRIAS, an underactuated bipedal robot, under different types of terrain, including changing step length in the range of

[23:78] cm; or changing both step length and step height in the range of [35:60] cm and [-22:22] cm respectively. For these experiments, we achieved dynamic walking with the average speed of 0.6 m/s.

ACKNOWLEDGEMENTS

We would like to give special thanks to Professor Jessy W. Grizzle and Xingye Da at the University of Michigan for their discussion and for generously sharing the optimization code of the MARLO robot. The preliminary experiment with on-board camera reported here have also benefited greatly from the participation of Allan Wang (Carnegie Mellon University). His work with the camera helps to estimate accurately the distance between the camera to stepping stones.

REFERENCES

Ames, A. D., Galloway, K., Sreenath, K. and Grizzle, J. W. (2014), 'Rapidly exponentially stabilizing control lyapunov functions and hybrid zero dynamics', *IEEE Transactions on Automatic Control (TAC)* **59**(4), 876–891.

Chestnutt, J., Kuffner, J., Nishiwaki, K. and Kagami, S. (2003), Planning biped navigation strategies in complex environments, *in* 'IEEE International Conference on Humanoid Robotics', pp. 117–123.

Chestnutt, J., Lau, M., Cheung, G., Kuffner, J., Hodgins, J. and Kanade, T. (2005), 'Footstep planning for the honda asimo humanoid', *Proceedings of the 2005 IEEE International Conference on Robotics and Automation.* pp. 629 – 634.

Da, X., Harib, O., Hartley, R., Griffin, B. and Grizzle, J. (2016), 'From 2d design of underactuated bipedal gaits to 3d implementation: Walking with speed tracking', *IEEE Access* **PP**(99), 1–1.

Da, X., Hartley, R. and Grizzle, J. W. (2017), First steps toward supervised learning for underactuated bipedal robot locomotion, with outdoor experiments on the wave field, *in* 'IEEE International Conference on Robotics and Automation (ICRA)'.

Dai, H., Valenzuela, A. and Tedrake, R. (2014), Whole-body motion planning with centroidal dynamics and full kinematics, *in* 'Humanoid Robots (Humanoids), 2014 14th IEEE-RAS International Conference on', IEEE, pp. 295–302.

Deits, R. L. H. (2014), Convex segmentation and mixed-integer footstep planning for a walking robot, Master's thesis, Massachusetts Institute of Technology.

Deits, R. and Tedrake, R. (2014), 'Footstep planning on uneven terrain with mixed-integer convex optimization.', *Proceedings of the 2014 IEEE/RAS International Conference on Humanoid Robots* pp. 279–286.

Desai, R. and Geyer, H. (2012), 'Robust swing leg placement under large disturbances', *Proceedings of the IEEE International Conference on Robotics and Biomimetics (ROBIO)* pp. 265–270.

Feng, S., Whitman, E., Xinjilefu, X. and Atkeson, C. G. (2015), 'Optimization-based full body control for the darpa robotics challenge', *Journal of Field Robotics* **32**(2), 293–312.

Gurriet, T., Finet, S., Boeris, G., Hereid, A., Harib, O., Masselin, M., Grizzle, J. and Ames, A. D. (2017), Towards restoring locomotion for paraplegics: Realizing dynamically stable walking on exoskeletons, *in* 'Submitted to 2018 IEEE International Conference on Robotics and Automation (ICRA)', IEEE.

Hereid, A., Cousineau, E. A., Hubicki, C. M. and Ames, A. D. (2016), 3d dynamic walking with underactuated humanoid robots: A direct collocation framework for optimizing hybrid zero dynamics, *in* '2016 IEEE International Conference on Robotics and Automation (ICRA)', IEEE, Stockholm, Sweden, pp. 1447–1454.

Hereid, A., Hubicki, C. M., Cousineau, E. A., Hurst, J. W. and Ames, A. D. (2015), Hybrid zero dynamics based multiple shooting optimization with applications to robotic walking, *in* '2015 IEEE International Conference on Robotics and Automation (ICRA)', IEEE, pp. 5734–5740.

Hubicki, C., Grimes, J., Jones, M., Renjewski, D., Spröwitz, A., Abate, A. and Hurst, J. (2016), 'Atrias: Design and validation of a tether-free 3d-capable spring-mass bipedal robot', *The International Journal of Robotics Research* **35**(12), 1497–1521.

Jones, M. S. (2014), Optimal control of an underactuated bipedal robot, Master's thesis, Oregon State University, ScholarsArchive@OSU.

Kajita, S., Kanehiro, F., Kaneko, K., Fujiwara, K., Harada, K., Yokoi, K. and Hirukawa, H. (2003), 'Biped walking pattern generation by using preview control of zero-moment point', *Proceedings of the IEEE International Conference on Robotics and Automation (ICRA)* **2**, 1620 – 1626.

Kuffner, J. J., Nishiwaki, K., Kagami, S., Inaba, M. and Inoue, H. (2001), 'Footstep planning among obstacles for biped robots', *Proceedings of the 2001 IEEE/RSJ International Conference on Intelligent Robots and Systems,* **1**, 500 – 505.

Kuindersma, S., Permenter, F. and Tedrake, R. (2014), An efficiently solvable quadratic program for stabilizing dynamic locomotion, *in* 'Robotics and Automation (ICRA), 2014 IEEE International Conference on', IEEE, pp. 2589–2594.

Michel, P., Chestnutt, J., Kuffner, J. and Kanade, T. (2005), Vision-guided humanoid footstep planning for dynamic environments, *in* 'Humanoids', pp. 13–18.

Motahar, M. S., Veer, S. and Poulakakis, I. (2016), Composing limit cycles for motion planning of 3d bipedal walkers, *in* 'the IEEE Conference On Decision and Control (CDC)'.

Nguyen, Q., Agrawal, A., Da, X., Martin, W. C., Geyer, H., Grizzle, J. W. and Sreenath, K. (2017), Dynamic walking on randomly-varying discrete terrain with one-step preview, *in* 'Robotics: Science and Systems (RSS)'.

Nguyen, Q., Da, X., Grizzle, J. W. and Sreenath, K. (2016), Dynamic walking on stepping stones with gait library and control barrier, *in* 'Workshop on Algorithimic Foundations of Robotics'.

Nishiwaki, K., Chestnutt, J. and Kagami, S. (2012), 'Autonomous navigation of a humanoid robot over unknown rough terrain using a laser range sensor', *The International Journal of Robotics Research* **31**(11), 1251–1262.

Press, W. H., Teukolsky, S. A., Vetterling, W. T. and Flannery, B. P. (1996), *Numerical recipes in C*, Vol. 2, Cambridge university press Cambridge.

Ramezani, A., Hurst, J. W., Akbari Hamed, K. and Grizzle, J. W. (2014), 'Performance Analysis and Feedback Control of ATRIAS, A Three-Dimensional Bipedal Robot', *Journal of Dynamic Systems, Measurement, and Control* **136**(2).

Rutschmann, M., Satzinger, B., Byl, M. and Byl, K. (2012), 'Nonlinear model predictive control for rough-terrain robot hopping', *Proceedings of the IEEE/RSJ International Conference on Intelligent Robots and Systems (IROS)* pp. 1859–1864.

Siravuru, A., Wang, A., Nguyen, Q. and Sreenath, K. (2017), Deep visual perception for dynamic walking on discrete terrain, *in* 'IEEE-RAS International Conference on Humanoid Robots'.

W-Prize (2009), 'The W-Prize on stepping stones', *http://www.wprize.org/SteppingStones.html* .

Westervelt, E. R., Grizzle, J. W., Chevallereau, C., Choi, J. and Morris, B. (2007), *Feedback Control of Dynamic Bipedal Robot Locomotion*, Control and Automation, CRC, Boca Raton, FL.

Yang, T., Westervelt, E., Serrani, A. and Schmiedeler, J. P. (2009), 'A framework for the control of stable aperiodic walking in underactuated planar bipeds', *Autonomous Robots* **27**(3), 277–290.